Effects of the legacy of axial cooling on partitioning of hydrothermal heat extraction from oceanic lithosphere

G. A. Spinelli[1] and R. N. Harris[2]

[1]   Water circulating through oceanic lithosphere extracts large quantities of heat, affecting magmatic, tectonic, geochemical, and microbial processes. Numerous estimates for the amount of hydrothermal heat extraction have been made on the basis of the difference between the predicted and observed heat flux across the seafloor. These methods have assumed a dynamic steady state thermal system. We show that this assumption is not warranted and leads to an incorrect partitioning of hydrothermal circulation between ridge axes and flanks. To more accurately estimate hydrothermal heat loss on ridge axes and flanks, we consider the spatial and temporal extent and vigor of axial hydrothermal circulation in calculating hydrothermal heat extraction. Axial fluid circulation perturbs the thermal state of oceanic lithosphere for ~5 Ma after that circulation ceases, reducing the hydrothermal heat extraction on ridge flanks. We find ~30% of hydrothermal heat extracted on axis, ~10% extracted near axis (from end of axial hydrothermal circulation to 1 Ma), and ~60% extracted from lithosphere >1 Ma.

Citation: Spinelli, G. A., and R. N. Harris (2011), Effects of the legacy of axial cooling on partitioning of hydrothermal heat extraction from oceanic lithosphere, *J. Geophys. Res.*, *116*, B09102, doi:10.1029/2011JB008248.

1.   Introduction

[2]   Hydrothermal circulation advects heat from the oceanic lithosphere to the overlying ocean. Evidence for fluid circulating through and extracting heat from oceanic lithosphere includes the presence of metalliferous sediment at mid-ocean ridges [*Bostrom and Peterson*, 1966; *Haymon et al.*, 2005], reduced magnetization with distance from mid-ocean ridge axes [*Irving et al.*, 1970; *Tivey and Johnson*, 2002], scattered and anomalously low seafloor heat flux at mid-ocean ridge axes and flanks [*Lister*, 1972; *Williams et al.*, 1974; *Davis et al.*, 1999], and direct observations of venting [*Corliss et al.*, 1979; *Baker and Massoth*, 1986; *Ramondenc et al.*, 2006]. In order to understand the Earth's thermal budget, lithospheric cooling, and processes affecting the evolution of oceanic lithosphere, numerous studies have sought to quantify the amount of heat extracted from the lithosphere by hydrothermal circulation [e.g., *Wolery and Sleep*, 1976; *Sclater et al.*, 1980; *Stein and Stein*, 1994; *Elderfield and Schultz*, 1996; *Mottl*, 2003]. Many of these studies distinguish between high-temperature axial hydrothermal circulation and low-temperature ridge flank circulation [e.g., *Mottl and Wheat*, 1994; *Elderfield and Schultz*, 1996; *Mottl*, 2003]. Often, these high- and low-temperature regimes are differentiated to facilitate estimates of geochemical fluxes [e.g., *Mottl and Wheat*, 1994] and to understand processes

controlling the alteration history of oceanic crust [*Cann and Gillis*, 2004].

[3]   Estimates of hydrothermal heat extraction from oceanic lithosphere commonly are derived from the difference between models and observations of conductive heat loss through the seafloor [*Wolery and Sleep*, 1976; *Sclater et al.*, 1980; *Stein and Stein*, 1994]. The discrepancy between these predicted values and the observations are inferred to result from fluid advecting heat from the lithosphere (Figure 1). In the absence of hydrothermal circulation, the predicted and observed heat fluxes should be equal barring other thermal perturbations. Hydrothermal circulation intercepts a portion of the predicted heat and advects it laterally away from regions of sediment cover where measurements are made. Because fluids advecting heat preferentially discharge through exposed basement where measurements are rare, heat flux measurements miss the advective component of the total heat flow. Global estimates of hydrothermal heat flux are based on the difference between global models of predicted heat flux and that actually observed [*Wolery and Sleep*, 1976; *Sclater et al.*, 1980; *Stein and Stein*, 1994]:

$$q_{hydrothermal} = q_{predicted} - q_{observed} \qquad (1)$$

[4]   This method for quantifying hydrothermal heat extraction has been applied to estimate both a total hydrothermal heat loss from oceanic lithosphere (~10–11 TW) and the distribution of that heat loss between mid-ocean ridge (i.e., axial), near-axis, and off-axis settings [e.g., *Sclater et al.*, 1980; *Stein and Stein*, 1994; *Stein et al.*, 1995; *Mottl*, 2003]. Accurate characterization of the partitioning of hydrothermal heat extraction between mid-ocean ridges and flanks has

---

[1]Earth and Environmental Science Department, New Mexico Institute of Mining and Technology, Socorro, New Mexico, USA.
[2]College of Oceanic and Atmospheric Science, Oregon State University, Corvallis, Oregon, USA.
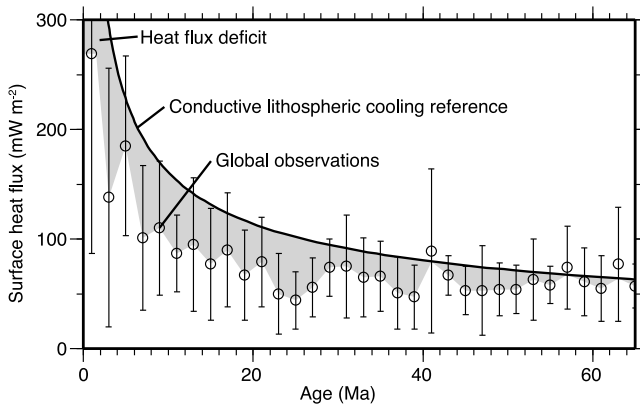
Figure 1. Heat flux versus age for oceanic lithosphere. Black line is predicted heat flux across seafloor for conductive cooling. Circles are average observed conductive heat flux grouped by lithospheric age for 2 Ma bins [*Stein and Stein*, 1993]; vertical lines extend ±1 standard deviation. Shaded area is heat flux deficit attributed to hydrothermal heat extraction.

implications for understanding controls on ocean chemistry, microbial processes, and the nature of heat transfer associated with spreading centers because these depend on accurate knowledge of hydrothermal fluxes [*Mottl and Wheat*, 1994; *Elderfield and Schultz*, 1996; *Mottl*, 2003]. In this study, we show that although using the difference between the predicted and observed surface heat flux is effective at determining the total hydrothermal heat loss, this method has significant, though previously underappreciated, limitations in quantifying the distribution of that heat loss. These limitations arise owing to changes in the depth of hydrothermal cooling between mid-ocean ridge axis and flank. We explore an alternate formulation for estimating the partitioning of hydrothermal circulation between near-axis and off-axis flow that incorporates estimates of the depth extent of circulation. This formulation is valid for mid-ocean ridges, ridge flanks, and older oceanic crust; it yields a new estimate for the distribution of hydrothermal heat flux.

2. Hydrothermal Circulation Depth

[5] Estimates for the depth of hydrothermal circulation at ridge axes are based on observations of the depth of microseismicity [*Toomey et al.*, 1988; *Kong et al.*, 1992; *Pelayo et al.*, 1994; *Golden et al.*, 2003; *Wilcock et al.*, 2002], alteration in ophiolites [*Gregory and Taylor*, 1981; *Cann and Gillis*, 2004], near-axis subsidence patterns [*Cochran and Buck*, 2001], thermal models [*Chen and Phipps Morgan*, 1996; *Cherkaoui et al.*, 2003; *Maclennan et al.*, 2005], and interpretation of seismic tomography [*Dunn et al.*, 2000]. Conservative estimates from microseismicity and seismic velocities suggest hydrothermal cooling at least through the pillow lavas and sheeted dikes to ~2 km depth [*Dunn and Toomey*, 2001; *Wilcock et al.*, 2002]. Similarly, alteration of crustal rocks in the Trodos ophiolite suggests axial hydrothermal cooling to the base of the sheeted dikes (~2 km depth) for crust formed at a fast spreading rate [*Cann and Gillis*, 2004]. For the Oman ophiolite, also fast spreading crust, oxygen and strontium isotope data indicate pervasive

fluid flow through the sheeted dikes and diminishing, channelized hydrothermal circulation through the underlying gabbro [*Cann and Gillis*, 2004; *Coogan et al.*, 2006]. Cooling rates for a crustal section of the Oman ophiolite calculated from closure temperatures for diffusive exchange of calcium from olivine indicate that the lower crust cools ~2–3 orders of magnitude slower than upper crust [*Coogan et al.*, 2007]. This and other evidence lead some to conclude that for fast spreading ridges the upper ~2 km of crust cools hydrothermally, but the lower crust cools conductively [*Cann and Gillis*, 2004; *Coogan et al.*, 2007]. However, calcium in olivine determined cooling rates from a different crustal section of Oman ophiolite (~100 km distant) indicate rapid cooling throughout the entire 6 km thickness of crust within 1–2 km of the ridge axis; this rapid cooling is interpreted to indicate hydrothermal circulation to ~6 km depth [*VanTongeren et al.*, 2008]. *VanTongeren et al.* [2008] suggest that anomalously slow cooling rates determined in the lower crust for the other Oman site [i.e., *Coogan et al.*, 2007] result from reheating of the base of that section by a dike swarm intruded into the mantle. Other estimates indicate near-ridge fluid circulation through the entire crustal thickness of ~6 km, with flow facilitated by thermal cracking through sheeted dikes into the underlying gabbro [*Wilcock and Delaney*, 1996]. Seismic velocities across the fast spreading East Pacific Rise are interpreted to indicate that the full crustal thickness is developed within a few kilometers of the ridge axis; this requires hydrothermal heat extraction to ~6 km depth [*Dunn et al.*, 2000].

[6] Hydrothermal circulation depth is likely greater for slow spreading crust than fast spreading crust. Earthquake locations are restricted to rocks cool enough for brittle failure; therefore, the locations of seismic events constrain the depth to the temperature-controlled brittle-ductile transition. Axial earthquakes are deeper at slow spreading ridges than at fast spreading ridges [*Huang and Solomon*, 1988]. At the slow spreading Mid-Atlantic Ridge, axial earthquakes occur at or below the base of the crust [*Toomey et al.*, 1988; *Kong et al.*, 1992]. At the intermediate spreading Juan de Fuca Ridge, axial microseismicity occurs at 2–4 km depth [*Golden et al.*, 2003; *Wilcock et al.*, 2002]. At the fast spreading East Pacific Rise, axial seismicity is restricted to the upper 1 km of crust [*Sohn et al.*, 1998, 1999]. In addition, the depth to zones of partial melt beneath mid-ocean ridges decreases with increasing spreading rate [*Purdy et al.*, 1992]. Finally, calcium in olivine determined cooling rates show rapid cooling of the entire ~6 km crustal section for slow spreading crust, but slower cooling rates below 2 km depth for fast spreading crust (at least in one crustal section) indicative of conductive cooling [*Coogan et al.*, 2007]. These trends lead *Fisher* [2003] to postulate that the depth of axial hydrothermal cooling decreases systematically with increasing spreading rate.

[7] In contrast to axial hydrothermal circulation, fluid flow through the flanks of mid-ocean ridges likely is restricted to a high-permeability aquifer composed of pillow lavas that comprise the upper ~600 m of the basement rock [*Becker and Davis*, 2004; *Fisher*, 1998]. The transition from deep axial to shallow off-axis hydrothermal circulation likely results from the cessation of active faulting and the sealing of fractures [*Cann and Gillis*, 2004]. The change in fluid circulation depth from ridge axis to flank has important consequences for
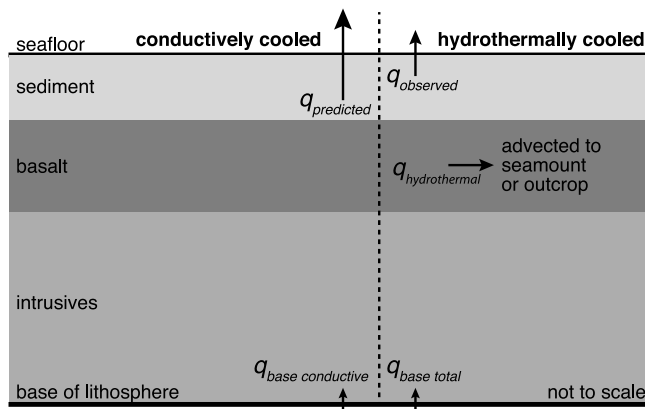
Figure 2. Heat fluxes into and out of oceanic lithosphere. Hypothetical lithosphere only cooled by conduction is shown left of dashed line. Typical oceanic lithosphere with some heat conducted through sediment to the seafloor and some heat extracted by hydrothermal circulation in a basaltic aquifer is shown right of dashed line.

determining the magnitude and age distribution of hydrothermal heat extraction.

3. Quantifying Hydrothermal Heat Extraction

[8] We quantify hydrothermal heat extraction by explicitly considering the depth evolution of geotherms as a function of time. We start by considering the change in plate heat content as a function of time and then link the formulation to the temporal evolution of geotherms. The conservation of energy dictates that the conductive and hydrothermal heat loss must be balanced by changes in the heat content of the plate. The temporal change in plate heat content due to hydrothermal circulation can be expressed as

$$\frac{\Delta H_{hydrothermal}}{\Delta t} = \frac{\Delta H_{total}}{\Delta t} - \frac{\Delta H_{conductive}}{\Delta t}, \qquad (2)$$

where ΔH_{total} is the combination of hydrothermal and conductive heat loss and $\Delta H_{conductive}$ is the conductive heat loss. The rate of change in heat content is controlled by the difference between the heat flux into the base of the plate and the heat flux out the top of the plate. For a conductively cooling plate, the change in heat content with time is

$$\frac{\Delta H_{conductive}}{\Delta t} = \left(q_{base\ conductive} - q_{predicted}\right)A, \qquad (3)$$

where $q_{base\ conductive}$ is the heat flux into the base of the plate, $q_{predicted}$ is the conductive flux out of the top of the plate (Figure 2), and A is the area of lithosphere for plate ages over the range Δt. With hydrothermal heat extraction in addition to heat conduction, the heat flux out the top of the plate is the observed surface heat flux plus the hydrothermal heat flux. Thus, the change in heat content with time is

$$\frac{\Delta H_{total}}{\Delta t} = \left(q_{base\ total} - \left(q_{observed} + q_{hydrothermal}\right)\right)A, \qquad (4)$$

where $q_{base\ total}$ is the heat flux into the base of a lithospheric plate with a shallow aquifer, $q_{hydrothermal}$ is the heat loss due

to hydrothermal circulation, and $q_{observed}$ is the conductive heat loss measured at the seafloor (Figure 2). Equations (3) and (4) are substituted into equation (2) and rearranged to solve for hydrothermal heat extraction:

$$q_{hydrothermal} = \left(q_{predicted} - q_{observed}\right) + \left(q_{base\ total} - q_{base\ conductive}\right)$$
$$- \frac{\Delta H_{total} - \Delta H_{conductive}}{A\Delta t}. \qquad (5)$$

Differences in the basal heat fluxes are extremely small (<1.5 mW m^{-2}) and may be ignored with little effect [*Sclater et al.*, 1980], yielding

$$q_{hydrothermal} = \left(q_{predicted} - q_{observed}\right) - \frac{\Delta H_{total} - \Delta H_{conductive}}{A\Delta t}. \qquad (6)$$

[9] Typical formulations calculating hydrothermal heat extraction from the surface heat flux anomaly [e.g., *Wolery and Sleep*, 1976; *Sclater et al.*, 1980; *Stein and Stein*, 1994] only include the first term on the right-hand side of equation (6). Implicit in these formulations is an assumption that the heat flux into the base of the shallow aquifer is equal to the expected surface heat flux ($q_{predicted}$) at all times. However, this is only true when the system is in a dynamic steady state (i.e., last term in equation (6) is zero). The last term in equation (6) accounts for conductive changes in geotherms that lag behind changes in circulation depth and efficiency. This term may be large on ridge axes and the flanks of mid-ocean ridges where the thermal state of the lithosphere adjusts to changes in the depth extent of hydrothermal circulation.

[10] To quantify hydrothermal heat flux, we link equation (6) to geotherms and depths of circulation by calculating the temporal change in heat content (ΔH_{total} and $\Delta H_{conductive}$) in the plate as

$$\frac{\Delta H}{\Delta t} = \rho c \int_A \frac{\Delta T}{\Delta t} dz, \qquad (7)$$

where ρ is lithospheric density (3330 kg m^{-3}), c is specific heat (1171 J kg^{-1} °C^{-1}) [*Parsons and Sclater*, 1977; *Stein and Stein*, 1994], and ΔT is the difference between geotherms at the beginning and end of an age interval (Figure 3). This formulation explicitly incorporates the depth extent of hydrothermal circulation. Figure 3 illustrates the thermal inertia following a reduction in the depth of hydrothermal circulation from the ridge axis to ridge flank environment. We show modeled geotherms for 0, 0.11, and 1 Ma. In the conductive case (Figure 3a), the lithosphere is only cooled by conduction to a constant temperature (0°C) seafloor. In the second case (Figure 3b), axial hydrothermal cooling penetrates to 6 km depth beginning at the ridge (0$^+$ Ma) and lasts until 0.11 Ma (i.e., 6 km from ridge for 5.5 cm yr^{-1} half-spreading rate). After 0.11 Ma, hydrothermal circulation is turned off and heat is only transported by conduction. From 0 to 0.11 Ma, the rate of heat loss from the conductively cooled plate is slower than for the hydrothermally cooled plate. In the transition from deep axial to conductive cooling (0.11–1 Ma), the rate of heat loss from the conductively cooled plate is faster than for hydrothermally cooled plate, as the hydrothermally perturbed
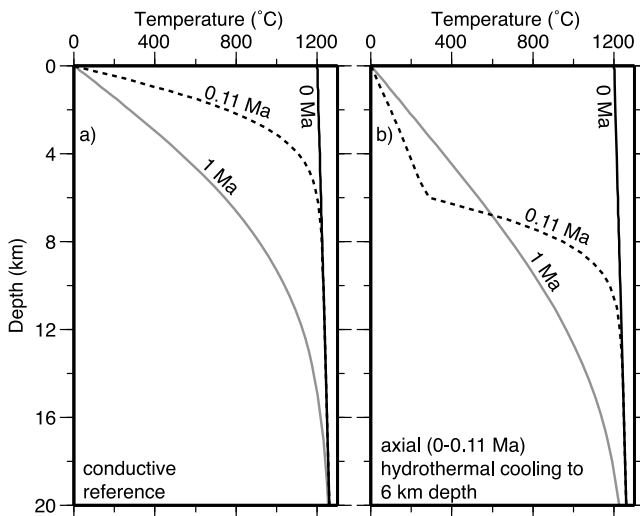
Figure 3. Example geotherms in oceanic lithosphere cooled by (a) conduction and (b) conduction plus axial hydrothermal circulation. In the hydrothermally cooled example, axial fluid circulation extends to 6 km depth and 6 km distance from the ridge (0–0.11 Ma for a half-spreading rate of 5.5 cm yr^{-1}). There is no hydrothermal heat extraction after 0.11 Ma. The difference between successive geotherms is used to calculate the temporal change in heat content in the plate.

geotherm conductively recovers. Following the cessation of axial hydrothermal circulation, some heat warms the upper lithosphere, decreasing the rate of heat loss from the plate. This example illustrates how the formulation in equation (1) would mischaracterize the partitioning between ridge axis and ridge flank hydrothermal circulation; hydrothermal circulation on the ridge axis would be underestimated and that on the ridge flank would be overestimated.

4. Numerical Models

[11] Our goal is to explore and estimate the partitioning between on- and off-axis hydrothermal heat loss as a function of the depth of axial hydrothermal circulation. We calculate the evolution of temperatures in oceanic lithosphere with a 2-D finite element model that accounts for heat conduction, movement of the plate away from a mid-ocean ridge, hydrothermal heat extraction from a prescribed aquifer, and sediment accumulation (Figure 4). Our plate is 95 km thick [*Stein and Stein*, 1994] with constant temperatures at the surface (0°C) and base of the plate (1330°C). Geotherms are initialized with temperatures at the ridge axis (0 Ma) increasing from 1200°C at the surface by 3°C km^{-1} to 33 km depth; below 33 km temperatures increase 0.3°C km^{-1} [*Morton and Sleep*, 1985; *Elderfield and Schultz*, 1996; *Mottl*, 2003]. Using these geologically reasonable ridge axis temperatures as a boundary condition yields predicted surface heat fluxes for the conductively cooled case that are between those from the established models of *Parsons and Sclater* [1977] and *Stein and Stein* [1994]. Material (and its associated heat) is advected away from the ridge axis at a half-spreading rate. We generate models with half-spreading rates between 0.5 and 7.5 cm yr^{-1}. For each spreading rate, we run simulations with and without hydrothermal cooling.

[12] We assume that the width of the axial hydrothermal circulation zone on each side of the ridge axis is equal to its depth, so that hydrothermal circulation on either side of the ridge axis has an aspect ratio of one. This aspect ratio is consistent with estimates for the extent of axial cooling for East Pacific Rise [*Dunn et al.*, 2000; *Cherkaoui et al.*, 2003; *Maclennan et al.*, 2005]. Beyond the distance for axial hydrothermal cooling, the geotherm is allowed to conductively relax, except for a 600 m thick isothermal aquifer maintained in the upper crust (Figure 4). For these simple models we assume the cessation of axial hydrothermal circulation occurs as a step. Temperature in the off-axis aquifer is set by the observed surface heat flux and the sediment thickness. On the ridge axis, there is no sediment and basement is in contact with the overlying ocean. Beyond the axial cooling zone, sediment accumulates at 5 m Ma^{-1} [*Spinelli et al.*, 2004]. Outside the axial hydrothermal circulation zone, the thermal conductivity of the lithospheric plate (excluding sediment) is set to 3.1 W m^{-1} °C^{-1} [*Stein and Stein*, 1994; *Parsons and Sclater*, 1977]; sediment thermal conduc-
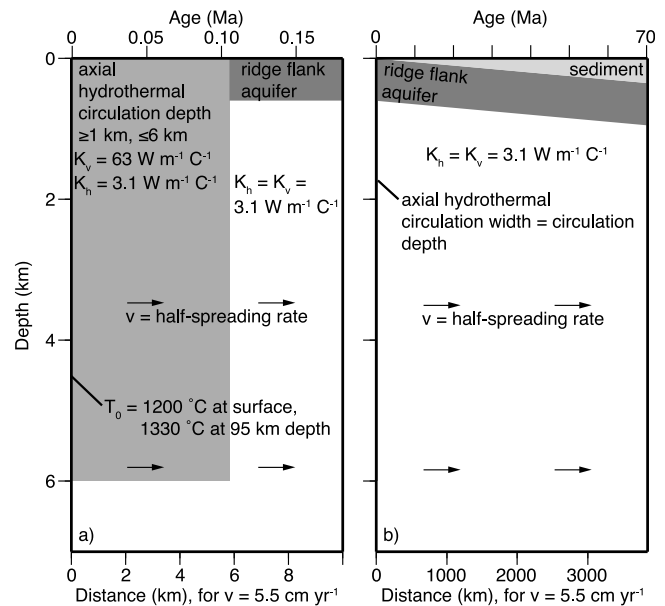

Figure 4. (a, b) Schematic cross sections of the numerical model used to evaluate oceanic lithosphere temperatures. The portion of the model near the mid-ocean ridge (Figure 4a) shows separate axial and ridge flank hydrothermal systems. Axial hydrothermal heat extraction is simulated by increasing the vertical thermal conductivity in some or all of the crust. The entire model extends from 0 to 70 Ma lithosphere (Figure 4b) and from the seafloor to 95 km depth (full depth range not shown for clarity; total horizontal distance depends on spreading rate). On the ridge flank, thermal gradients through seafloor sediment are specified on the basis of observed surface heat fluxes. The basaltic ridge flank aquifer is maintained at the basal sediment temperatures; below the ridge flank aquifer, heat conduction is the dominant process. Throughout the model, heat is advected laterally toward older lithosphere at the half-spreading rate; this advects heat away from the mid-ocean ridge and across the ridge-to-ridge flank transition.

Table 1. Model Parameters

Parameter	Value
Axial hydrothermal cooling depth (km)	1–6
Ridge flank hydrothermal cooling depth (km)	0.6
Plate thickness (km)	95
Seafloor temperature (°C)	0
Basal temperature (°C)	1330
Thermal conductivity of lithosphere, excluding sediment (W m^{-1} °C^{-1})	3.1
Thermal conductivity of sediment (W m^{-1} °C^{-1})	1.0
Density of lithosphere (kg m^{-3})	3330
Specific heat of lithosphere (J kg^{-1} °C^{-1})	1171

tivity is 1.0 W m^{-1} °C^{-1} [*Davis et al.*, 1997b, 1999]. Model parameters are summarized in Table 1.

[13] We simulate the thermal effect of axial hydrothermal heat extraction by increasing the vertical thermal conductivity over the depth of circulation by a factor of 20. This high thermal conductivity proxy for hydrothermal circulation has been successfully used in a number of studies [*Chen and Phipps Morgan*, 1996; *Davis et al.*, 1997a; *Cochran and Buck*, 2001]. To examine the efficacy of using this proxy for high Nusselt number circulation on the ridge axis, we compare geotherms at the axis-to-flank transition from our simulation and more detailed thermal models (Figure 5). *Cherkaoui et al.* [2003] and *Maclennan et al.* [2005] developed models for cooling of the lithosphere formed at the East Pacific Rise at ~9°N; their simulations include hydrothermal cooling through the entire 6 km thick crustal section. Our simulation, with the appropriate half-spreading rate of 5.5 cm yr^{-1} and an enhanced thermal conductivity to 6 km
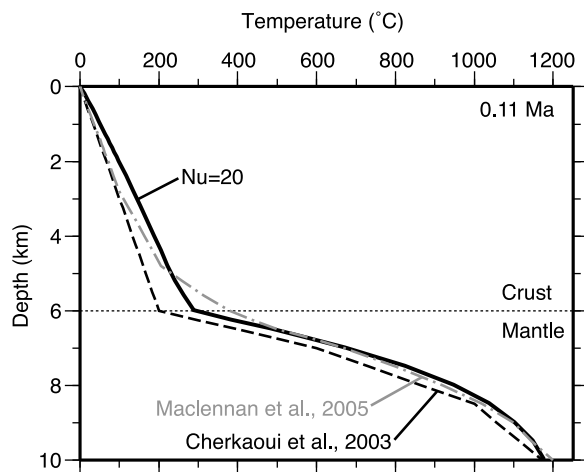
depth yields temperatures at 6 km off axis that are slightly warmer than the more detailed models (Figure 5) [*Cherkaoui et al.*, 2003; *Maclennan et al.*, 2005]. Thus, the high-conductivity proxy provides a conservative estimate of the effects of axial hydrothermal cooling in this case. An advantage of this technique is that it can be applied over the range of spreading rates and cooling depths that we examine, but for which detailed numerical models have not been developed. For the off-axis aquifer, the thermal effect of hydrothermal cooling is defined by using the observed surface heat flux to delineate a geotherm through the seafloor sediment; we define the ocean crust aquifer as a 600 m thick isothermal unit with temperature equal to the base of the sediment section. Therefore, the high-conductivity proxy is not applied, nor necessary, for the off-axis aquifer.

5. Results

[14] Figure 6 shows heat flux versus age resulting from different spreading rates and axial circulation depths of 2 and 6 km. Each curve starts where axial hydrothermal circulation conditions end. The conductive reference model and globally
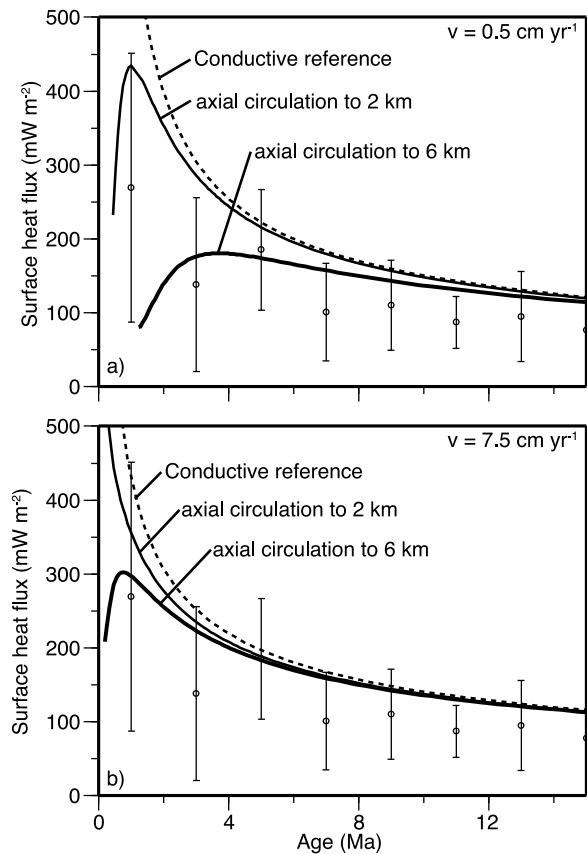

Figure 5. Modeled geotherms for fast spreading (5.5 cm yr^{-1} half-spreading rate) oceanic lithosphere 0.11 Ma after formation, in the transition from axial to off-axis hydrothermal circulation. Using a high-conductivity proxy for high Nusselt number (*Nu*) circulation in the crust (solid line) yields a slightly warmer geotherm than do other models of axial cooling (dashed lines); this warmer geotherm provides a conservative estimate of the effects of axial hydrothermal circulation on ridge flank surface heat flux.

Figure 6. Heat flux versus age for oceanic lithosphere, where lines are modeled heat flux with half-spreading rates of (a) 0.5 cm yr^{-1} and (b) 7.5 cm yr^{-1}. Circles are average observations for global data in 2 Ma bins; error bars are ±1 standard deviation. Dashed line is predicted seafloor heat flux for conductive cooling. Lower lines show modeled surface heat flux for conductive ridge flank cooling following axial hydrothermal cooling (no ridge flank hydrothermal heat extraction).
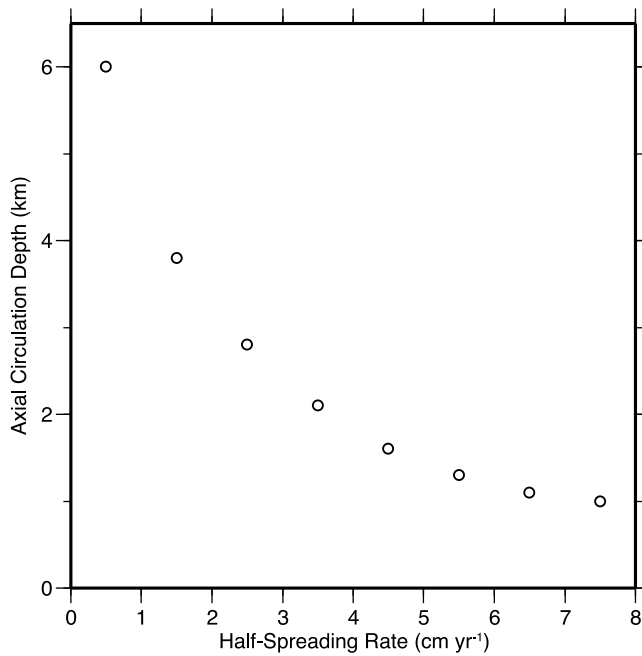
Figure 7. Axial hydrothermal cooling depth as a function of half-spreading rate for one set of simulations. In two other sets of simulations, axial hydrothermal cooling depth is 2 km or 6 km for all half-spreading rates.

averaged heat flow observations are also plotted for reference. Because the lateral extent of axial cooling is prescribed in terms of distance, the discrepancy is largest for slow spreading lithosphere. The thermal legacy of axial hydrothermal cooling to 2 km depth is smaller; surface heat flux approaches that predicted for a conductively cooled plate by ~3 Ma. The legacy of axial hydrothermal cooling affects surface heat flux from lithosphere younger than 3 Ma in cases with deep or shallow axial hydrothermal cooling and all spreading rates. These results confirm the functional relationships evident in equation (6); the long-lasting effect of axial hydrothermal cooling is proportional to its depth and inversely related to the spreading rate. The globally averaged heat flow data fall below our calculations of axial hydrothermal heat extraction even for the deepest circulation and slowest crust indicating the importance of hydrothermal heat flow on ridge flanks.

[15] We estimate the age distribution of global hydrothermal heat extraction accounting for variations in hydrothermal cooling depth by using equations (6) and (7). In the first two scenarios, axial hydrothermal cooling extends to either 2 km or 6 km. In a third set of simulations, the axial hydrothermal cooling depth decreases with increasing spreading rate. In these simulations, the depth of enhanced axial cooling is 6.0, 3.8, 2.8, 2.1, 1.6, 1.3, 1.1, and 1.0 km for crust formed at spreading rates of 0.5, 1.5, 2.5, 3.5, 4.5, 5.5, 6.5, and 7.5 cm yr^{-1}, respectively (Figure 7). To allow comparison with previous estimates, we determine amounts of hydrothermal heat extraction from the ridge axis and in 2 million year wide bins off axis. Specifically, we calculate hydrothermal heat flux (1) from the ridge axis (0 Ma) to the end of axial hydrothermal circulation, (2) from that axis-to-flank transition to 1 Ma, (3) from 1 Ma to 2 Ma, and (4) from 2 Ma

wide bins from 2 Ma to 70 Ma. The area for each age bin (used in equation (6)) is determined from the spreading rate and the length of the global mid-ocean ridge system spreading at that rate [*Baker and German*, 2004]. For age bins near the ridge, with set distances rather than ages, we calculate the predicted surface heat flux for each bin for all spreading rates, then determine average values weighted by the fractions of the total axial and near-axis areas for each spreading rate. We use the calculated hydrothermal heat flux and areas for each age bin and spreading rate combination to calculate the hydrothermal heat extracted. For each age bin, we sum both the hydrothermal heat and the area for all spreading rates. Finally, we calculate a global average hydrothermal heat flux for each age bin from the summed hydrothermal heat fluxes and areas. This provides our preferred estimates for the global hydrothermal heat flux distribution, accounting for differences in spreading rate. A limitation of this study is that we do not account for temporal changes in spreading rate, a complexity observed in oceanic lithosphere [*Muller et al.*, 2008]. Therefore, we scale the lithospheric area estimated from spreading rates and lengths of ridge to the area for 0–70 Ma lithosphere determined by *Muller et al.* [2008] in estimating the cumulative hydrothermal heat extraction from oceanic lithosphere.

[16] On axis we calculate hydrothermal heat fluxes 2.3–2.8 times larger than estimated from the difference between the predicted and observed surface heat fluxes alone (Figure 8). From the end of axial hydrothermal cooling to 6 Ma, we find substantially lower heat extraction by fluid circulation than estimated from the difference between predicted and observed surface heat fluxes. We illustrate this point by plotting hydrothermal heat extraction relative to that predicted from equation (1) (Figure 9). With axial circulation
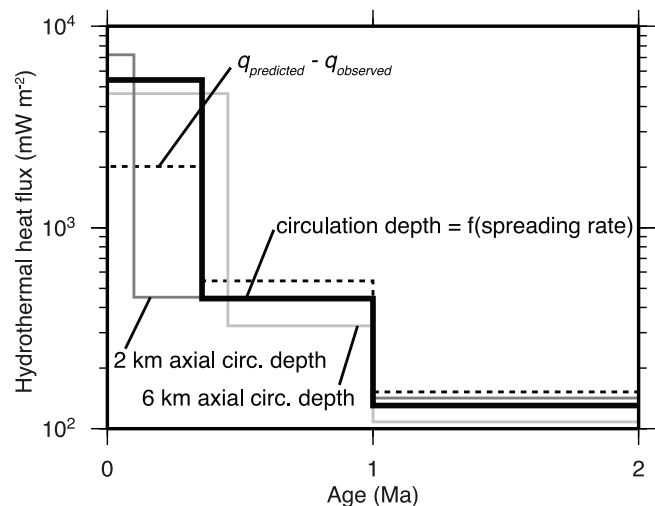

Figure 8. Hydrothermal heat flux versus age on and near axis calculated from the difference between predicted and observed surface heat flux (dashed line) and this study examining changes in lithospheric heat content (solid lines). The preferred model has decreasing axial hydrothermal circulation depth with increasing spreading rate (bold black line). The difference between predicted and observed surface heat flux underestimates axial hydrothermal heat extraction and overestimates near-axis hydrothermal heat extraction.
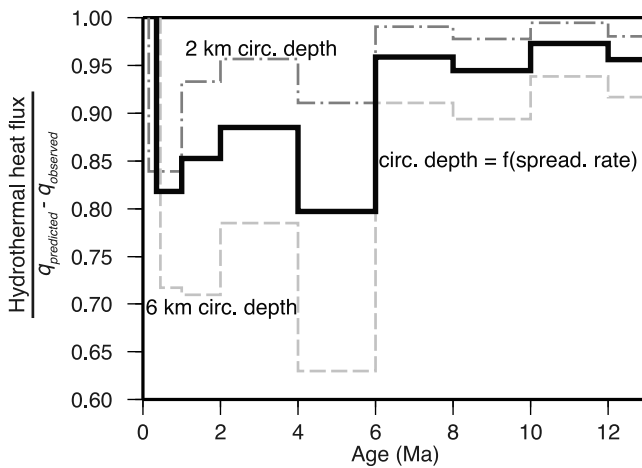
Figure 9. Hydrothermal heat flux normalized to the difference between predicted and observed surface heat flux. In the preferred model (bold line), hydrothermal heat flux on the ridge flank from 0.36 to 6 Ma averages 84% of that estimated from the difference between predicted and observed surface heat flux. For lithosphere >10 Ma, hydrothermal heat extraction in all scenarios is within 10% of the estimate from predicted and observed heat fluxes.

extending to 6 km depth for all spreading rates, ridge flank hydrothermal heat extraction until 6 Ma is 71% of that determined from equation (1). If axial hydrothermal cooling is limited to 2 km depth and 2 km from the ridge, ridge flank hydrothermal cooling to 6 Ma is 92% of that determined from equation (1). This shallow and narrowly distributed axial hydrothermal cooling is an extreme minimum. With axial circulation extending to 6 km depth, but limited to the area within 2 km of the ridge, ridge flank hydrothermal cooling to 6 Ma is 84% of that determined from equation (1). In our preferred model, on-axis circulation depth decreases from 6 km for the slowest spreading to 1 km for the fastest spreading case. In this scenario, axial hydrothermal cooling is 2.7 times larger than estimated from equation (1); ridge flank hydrothermal cooling to 6 Ma averages 84% of that determined from equation (1). After 6 Ma our calculated hydrothermal heat fluxes rapidly approach those determined from the difference between the predicted and observed surface heat fluxes.

6. Discussion

[17] As hydrothermal circulation transitions from deeply circulating fluids characteristic of ridge axes to shallow circulation patterns off axes, the rebound of temperatures in the shallow lithosphere lags behind the change in circulation style at a rate governed by conductive time constants (Figure 6). Calculating hydrothermal heat flux from the difference between the predicted and observed surface heat flux assumes that the surface heat flux is depressed only owing to current hydrothermal conditions. This is true only if conductive heat transfer can keep up with changes in hydrothermal circulation depth and vigor. With the simplistic approach inherent in equation (1), some of the surface heat flux anomaly on ridge flanks could be mistaken for local

advective heat loss [*Fisher*, 2003], although the heat was already extracted near the ridge. Accounting for changes in hydrothermal circulation depth shows that more heat is extracted from the ridge axis and less heat is extracted from the young ridge flank than previously recognized. In our preferred scenario where the axial circulation depth is a function of spreading rate, one quarter of all hydrothermal heat from ocean lithosphere is extracted on axis (Table 2). Although this is a large redistribution in the location of hydrothermal heat extraction, the majority still occurs on flanks and older lithosphere.

[18] We have guided our analysis using globally averaged heat flux data and models, in part because we are focusing on global relationships and in part because closely spaced heat flux observations along profiles covering the ridge axis and young ridge flank are rare. One location where these data exist is the East Pacific Rise near 9° N. Observed heat flux and seismic structure document the extent of axial hydrothermal cooling and indicate an axial depth of circulation of about 6 km [*Dunn et al.*, 2000]. Heat flux data provide some insight into the combined effects of both axial and ridge flank hydrothermal cooling (Figure 10). Individual heat flux measurements are consistently lower than conductive cooling models predict, indicating persistent and ongoing hydrothermal circulation [*Von Herzen and Uyeda*, 1963; *Langseth et al.*, 1965]. These heat flux values also show considerable scatter due to variability in the local environmental parameters such as sediment thickness, extent of basement exposure, and three-dimensional permeability variations. To diminish this local variability, we average the data in 2 Ma age bins. We illustrate the predicted thermal legacy of axial circulation in this setting by showing results from a simulation with axial hydrothermal cooling (0–6 km from ridge; 0–0.11 Ma), but no ridge flank hydrothermal cooling (Figure 10a). The difference between the surface heat flux in the predicted (i.e., conductive) case and the case without ridge flank circulation is due entirely to axial hydrothermal circulation. The greatest discrepancy from the conductive prediction is at the end of axial hydrothermal cooling period. After axial hydrothermal circulation ceases, the curve rebounds somewhat but remains depressed relative to the conductive reference for considerable time. Our model results indicate that for the East Pacific Rise axial cooling, shallow geotherms are perturbed for at least 5 Ma after axial hydrothermal cooling ceases. Much of the low surface heat flux from lithosphere younger than 3 Ma attributed to ridge flank hydrothermal heat extraction based on the difference between $q_{predicted}$ and $q_{observed}$ reflects axial hydrothermal cooling (Figure 10b). This local analysis is consistent with and supports our global modeling results.

Table 2. Percentages of Total Hydrothermal Heat Flux

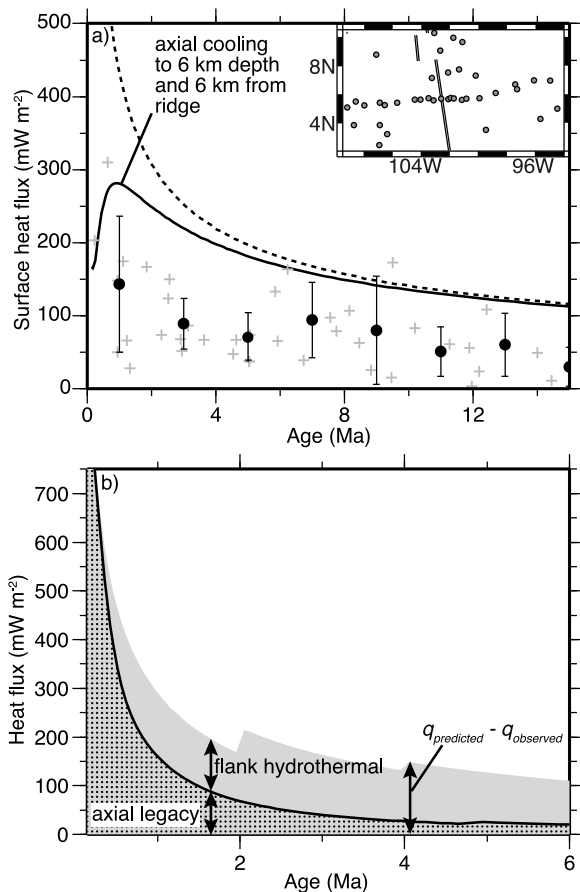| Age (Ma)	$q_{predicted} - q_{observed}$	This Study	This Study Including Hydrothermal Removal of 1 TW Latent Heat on Axis
0–0.356	9	22	29
0.356–1	16	12	11
1–2	5	4	4
2–4	11	9	8
>4	60	53	48

Figure 10. (a) Surface heat flux versus age on the flanks of the East Pacific Rise (EPR). Pluses are observations; circles are averages in 2 Ma bins; and error bars are ±1 standard deviation. Lines are modeled heat flux with a half-spreading rate of 5.5 cm yr^{-1}. Dashed line is predicted seafloor heat flux for conductive cooling. Solid line is modeled surface heat flux for conductive ridge flank cooling following axial hydrothermal cooling. Inset map shows surface heat flux observation (circles) on the flanks of the EPR; lines are ridge axis. (b) Hydrothermal heat flux and legacy of axial cooling on the flanks of the EPR. Shaded region (including under the stippled zone) is difference between predicted and observed surface heat flux. Stippled region is difference between predicted surface heat flux with only conductive cooling and with enhanced axial cooling to 6 km depth and 6 km distance from ridge (0.11 Ma for 5.5 cm yr^{-1} half-spreading rate). Ridge flank hydrothermal heat extraction is the shaded area above the stippled region. Steps in top of shaded region are due to single (average) values used for observed heat flux for discrete age bins.

[19] Figure 11 shows the percentage of axial hydrothermal heat extraction as a function of circulation depth and spreading rate. Similar to Figure 6, Figure 11 shows that axial hydrothermal heat extraction is proportional to the depth of axial circulation and the time for which axial circulation persists. However, Figure 11 also shows second-order effects not immediately obvious from Figure 6. For shallow axial circulation depths, the percentage of axial heat is relatively

independent of the spreading rate (Figure 11). In this region, hydrothermal extraction is minimal and conductive heat transfer into the axial hydrothermal circulation zone almost keeps pace with advective heat removal. For axial circulation deeper than ~4 km, hydrothermal heat extraction is less sensitive to the depth of circulation (Figure 11). This implies that fluids are removing heat much faster than it can be supplied by conductive heat transfer.

[20] Others have examined the thermal legacy of axial fluid circulation; this study builds on their basic observations. *Lister* [1972] estimated a potential legacy of axial hydrothermal cooling for the Juan de Fuca Ridge lasting ~2.5 Ma. His focus was to show that observed low heat flux values on the ridge flank (beyond 2.5 Ma) could not be explained on the basis of cooling at the ridge [*Lister*, 1972]. This study was instrumental in establishing the importance of ridge flank hydrothermal cooling, but little attention was paid to the first few million years of lithospheric heat transport. *Fisher* [2003] showed that a fraction of the heat flux deficit on very young lithosphere could result from the legacy of axial hydrothermal cooling. He estimated ~90% recovery from axial hydrothermal cooling by about 1 million years for most cases [*Fisher*, 2003]. *Fisher* [2003] used a 1-D model with no cooling below the hydrothermally cooled layer on axis; our simulations do not include either of these limitations.

[21] Our calculations of hydrothermal heat extraction from equations (6) and (7) only include heat associated with lowering the temperature of the lithosphere; they do not include extraction of any latent heat on axis. On the basis of crustal thickness and the latent heat of crystallization, *Elderfield and Schultz* [1996] and *Mottl* [2003] estimate ~1 TW of latent heat extracted on axis. Including the removal of this latent heat on axis further shifts the distribution of hydrothermal
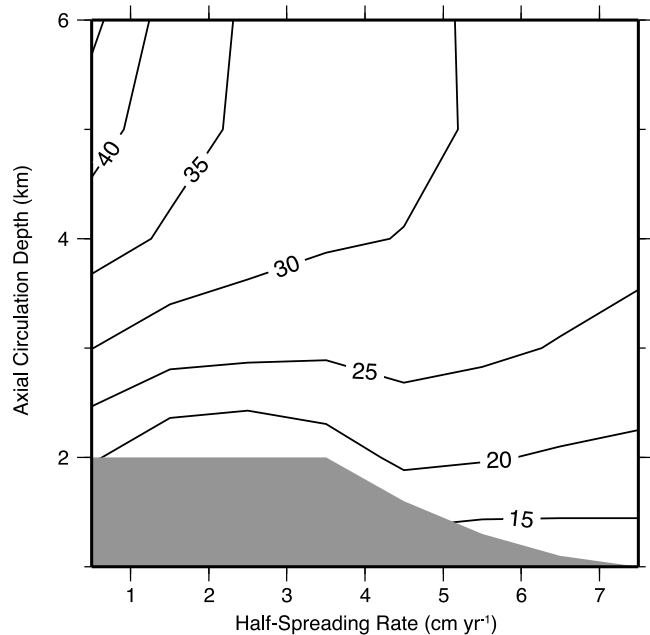

Figure 11. Percentage of hydrothermal heat extraction (total = 9.0 TW) occurring on axis as a function of half-spreading rate and axial circulation depth. Shaded area is outside the limits examined.
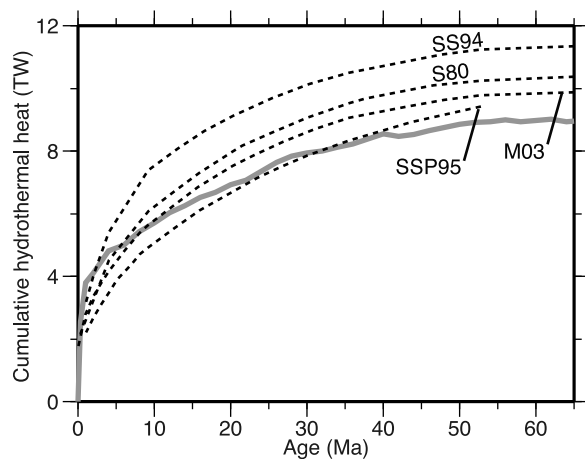
Figure 12. Cumulative hydrothermal heat extraction from oceanic lithosphere from this study (gray line) and previous studies (dashed lines): S80, *Sclater et al.* [1980]; SS94, *Stein and Stein* [1994]; SSP95, *Stein et al.* [1995]; and M03, *Mottl* [2003]. This study finds a greater proportion of hydrothermal heat extraction on axis and less hydrothermal heat extraction on young ridge flanks. Most hydrothermal heat extraction is from lithosphere >4 Ma.

heat extraction, with nearly one third of hydrothermal heat extracted on axis (Table 2).

[22] It is important to note that our results indicate a redistribution of hydrothermal heat extraction not a net increase or decrease from the entire oceanic lithosphere. In our preferred scenario, including 1 TW of latent heat extracted hydrothermally on axis, we estimate 9.0 TW of hydrothermal heat extraction from 0 to 65 Ma lithosphere (Figure 12). The most important distinction of our estimate for cumulative hydrothermal heat extraction relative to previous estimates is the difference in shape. The lower total value determined here results from three main factors. First, previous estimates of area [e.g., *Sclater et al.*, 1980; *Stein and Stein*, 1994] for 0–65 Ma lithosphere are nearly 10% larger than values determined from *Muller et al.* [2008]; using the larger area estimates would increase our total estimate by 0.7 TW, eliminating much of the discrepancy for the cumulative total values in Figure 12. Second, we use the observed surface heat flux from *Stein and Stein* [1993] that is divided into 2 Ma bins; their value for the 0–2 Ma bin is lower than that reported by *Stein and Stein* [1994], who used a smaller number of bins with an irregular age interval. Third, the temperatures we use at the axial and basal boundaries are slightly lower than those of *Stein and Stein* [1994].

[23] Fluid flux estimates through ocean lithosphere depend directly on estimates of hydrothermal heat extraction [e.g., *Mottl and Wheat*, 1994; *Elderfield and Schultz*, 1996; *Mottl*, 2003]. Our results suggest that fluid flux estimates based on earlier calculations of hydrothermal heat [e.g., *Sclater et al.*, 1980; *Stein and Stein*, 1994; *Elderfield and Schultz*, 1996; *Mottl*, 2003] underestimate high-temperature axial fluxes and overestimate low-temperature ridge flank flux (to ~5 Ma). Because hydrothermal heat flux estimates on mid-ocean ridges and flanks depend strongly on axial circulation depth, site-specific estimates for the actual depth of near-

ridge hydrothermal circulation are critical for characterizing particular locations and processes.

7. Conclusions

[24] Standard calculations of hydrothermal heat extraction from oceanic lithosphere based on the difference between the predicted and observed seafloor heat flux assume a dynamic steady state thermal system. This assumption is inappropriate in and around regions where hydrothermal circulation depth and/or vigor change, for example on mid-ocean ridge axes and flanks. When changes in hydrothermal circulation depth between ridge axes and flanks are considered, we find ~30% of hydrothermal heat extracted on axis, ~10% near axis (from end of axial hydrothermal circulation to 1 Ma), and ~60% from lithosphere >1 Ma. This is a much greater proportion of hydrothermal heat extracted on axis than would be determined from only the difference between the predicted and observed heat flux (~10% on axis). Estimates of fluid and chemical fluxes from ridge axes and flanks should be based on estimates of hydrothermal heat fluxes that account for temporal changes in hydrothermal circulation depth and vigor. Finally, we estimate 9.0 TW of cumulative hydrothermal heat extraction from 0 to 65 Ma lithosphere. This estimate is slightly lower than previous estimates, largely owing to improved estimates for ocean lithosphere area in this age range.

References

Baker, E. T., and C. R. German (2004), On the global distribution of hydrothermal vent fields, in *Mid-Ocean Ridges: Hydrothermal Interactions Between the Lithosphere and Oceans, Geophys. Monogr. Ser.*, vol. 148, edited by C. R. German, J. Lin, and L. M. Parson, pp. 245–266, AGU, Washington, D. C.

Baker, E. T., and G. J. Massoth (1986), Hydrothermal plume measurements: A regional perspective, *Science*, *234*, 980–982, doi:10.1126/science.234.4779.980.

Becker, K., and E. E. Davis (2004), In situ determinations of the permeability of the igneous ocean crust, in *Hydrogeology of the Oceanic Lithosphere*, edited by E. E. Davis and H. Elderfield, pp. 189–224, Cambridge Univ. Press, New York.

Bostrom, K., and M. N. A. Peterson (1966), Precipitates from hydrothermal exhalations on the East Pacific Rise, *Econ. Geol.*, *61*, 1258–1265, doi:10.2113/gsecongeo.61.7.1258.

Cann, J., and K. Gillis (2004), Hydrothermal insights from the Trodos ophiolite, Cyprus, in *Hydrogeology of the Oceanic Lithosphere*, edited by E. E. Davis and H. Elderfield, pp. 272–310, Cambridge Univ. Press, New York.

Chen, Y. J., and J. Phipps Morgan (1996), The effects of spreading rate, the magma budget, and the geometry of magma emplacement on the axial heat flux at mid-ocean ridges, *J. Geophys. Res.*, *101*, 11,475–11,482, doi:10.1029/96JB00330.

Cherkaoui, A. S. M., W. S. D. Wilcock, R. A. Dunn, and D. R. Toomey (2003), A numerical model of hydrothermal cooling and crustal accretion at a fast spreading mid-ocean ridge, *Geochem. Geophys. Geosyst.*, *4*(9), 8616, doi:10.1029/2001GC000215.

Cochran, J. R., and W. R. Buck (2001), Near-axis subsidence rates, hydrothermal circulation, and thermal structure of mid-ocean ridge crests, *J. Geophys. Res.*, *106*, 19,233–19,258, doi:10.1029/2001JB000379.

Coogan, L. A., K. A. Howard, K. M. Gillis, M. J. Bickle, H. Chapman, A. J. Boyce, G. R. T. Jenkin, and R. N. Wilson (2006), Chemical and

thermal constraints on focused fluid flow in the lower oceanic crust, *Am. J. Sci.*, 306, 389–427, doi:10.2475/06.2006.01.

Coogan, L. A., G. R. T. Jenkins, and R. N. Wilson (2007), Contrasting cooling rates in the lower oceanic crust at fast- and slow-spreading ridges revealed by geospeedometry, *J. Petrol.*, 48(11), 2211–2231, doi:10.1093/petrology/egm057.

Corliss, J. B., et al. (1979), Submarine thermal springs on the Galapagos rift, *Science*, 203, 1073–1083, doi:10.1126/science.203.4385.1073.

Davis, E. E., K. Wang, J. He, D. Chapman, H. Villinger, and A. Rosenberger (1997a), An unequivocal case for high Nusselt number hydrothermal convection in sediment-buried igneous oceanic crust, *Earth Planet. Sci. Lett.*, 146, 137–150, doi:10.1016/S0012-821X(96)00212-9.

Davis, E. E., A. T. Fisher, and J. Firth (1997b), *Proceedings of the Ocean Drilling Program: Initial Reports*, vol. 168, 470 pp., Ocean Drill. Program, College Station, Tex.

Davis, E. E., D. S. Chapman, K. Wang, H. Villinger, A. T. Fisher, S. W. Robinson, J. Grigel, D. Pribnow, J. Stein, and K. Becker (1999), Regional heat flow variations across the sedimented Juan de Fuca Ridge eastern flank: Constraints on lithospheric cooling and lateral hydrothermal heat transport, *J. Geophys. Res.*, 104, 17,675–17,688, doi:10.1029/1999JB900124.

Dunn, R. A., and D. R. Toomey (2001), Crack-induced seismic anisotropy in the oceanic crust across the East Pacific Rise (9°30′N), *Earth Planet. Sci. Lett.*, 189, 9–17, doi:10.1016/S0012-821X(01)00353-3.

Dunn, R. A., D. R. Toomey, and S. C. Solomon (2000), Three-dimensional seismic structure and physical properties of the crust and shallow mantle beneath the East Pacific Rise at 9°30′N, *J. Geophys. Res.*, 105, 23,537–23,555, doi:10.1029/2000JB900210.

Elderfield, H., and A. Schultz (1996), Mid-ocean ridge hydrothermal fluxes and the chemical composition of the ocean, *Annu. Rev. Earth Planet. Sci.*, 24, 191–224, doi:10.1146/annurev.earth.24.1.191.

Fisher, A. T. (1998), Permeability within basaltic oceanic crust, *Rev. Geophys.*, 36, 143–182, doi:10.1029/97RG02916.

Fisher, A. T. (2003), Geophysical constraints on hydrothermal circulation: Observations and models, in *Energy and Mass Transfer in Marine Hydrothermal Systems*, edited by P. E. Halbach, V. Tunnicliffe, and J. R. Hein, pp. 29–52, Dahlem Univ. Press, Berlin.

Golden, C. E., S. C. Webb, and R. A. Sohn (2003), Hydrothermal microearthquake swarms beneath active vents at Middle Valley, northern Juan de Fuca Ridge, *J. Geophys. Res.*, 108(B1), 2027, doi:10.1029/2001JB000226.

Gregory, R. T., and H. P. Taylor (1981), An oxygen isotope profile in a section of Cretaceous oceanic crust, Samail Ophiolite, Oman: Evidence for $\delta^{18}O$ buffering of the oceans by deep (>5 km) seawater-hydrothermal circulation at mid-ocean ridges, *J. Geophys. Res.*, 86, 2737–2755, doi:10.1029/JB086iB04p02737.

Haymon, R. M., K. C. Macdonald, S. B. Benjamin, and C. J. Ehrhardt (2005), Manifestations of hydrothermal discharge from young abyssal hills on the fast-spreading East Pacific Rise flank, *Geology*, 33, 153–156, doi:10.1130/G21058.1.

Huang, P. Y., and S. C. Solomon (1988), Centroid depths of mid-ocean ridge earthquakes: Dependence on spreading rate, *J. Geophys. Res.*, 93, 13,445–13,477, doi:10.1029/JB093iB11p13445.

Irving, E., J. K. Park, S. E. Haggerty, F. Aumento, and B. Loncarevic (1970), Magnetism and opaque mineralogy of basalts from the Mid-Atlantic Ridge at 45°N, *Nature*, 228, 974–976, doi:10.1038/228974a0.

Kong, L. S. L., S. C. Solomon, and G. M. Purdy (1992), Microearthquake characteristics of a mid-ocean ridge along-axis high, *J. Geophys. Res.*, 97, 1659–1685, doi:10.1029/91JB02566.

Langseth, M. G., P. J. Grim, and M. Ewing (1965), Heat flow measurements in the East Pacific Ocean, *J. Geophys. Res.*, 70, 367–380, doi:10.1029/JZ070i002p00367.

Lister, C. R. B. (1972), On the thermal balance of a mid-ocean ridge, *J. R. Astron. Soc.*, 26, 515–535.

Maclennan, J., T. Hulme, and S. C. Singh (2005), Cooling of the lower oceanic crust, *Geology*, 33, 357–360, doi:10.1130/G21207.1.

Morton, J. L., and N. H. Sleep (1985), A mid-ocean ridge thermal model: Constraints on the volume of axial hydrothermal heat flux, *J. Geophys. Res.*, 90, 11,345–11,353, doi:10.1029/JB090iB13p11345.

Mottl, M. J. (2003), Partitioning of energy and mass fluxes between mid-ocean ridge axes and flanks at high and low temperature, in *Energy and Mass Transfer in Marine Hydrothermal Systems*, edited by P. E. Halbach, V. Tunnicliffe, and J. R. Hein, pp. 271–286, Dahlem Univ. Press, Berlin.

Mottl, M. J., and C. G. Wheat (1994), Hydrothermal circulation through mid-ocean ridge flanks: Fluxes of heat and magnesium, *Geochim. Cosmochim. Acta*, 58, 2225–2237, doi:10.1016/0016-7037(94)90007-8.

Muller, R. D., M. Sdrolias, C. Gaina, and W. R. Roest (2008), Age, spreading rates, and spreading asymmetry of the world's ocean crust, *Geochem. Geophys. Geosyst.*, 9, Q04006, doi:10.1029/2007GC001743.

Parsons, B., and J. G. Sclater (1977), Analysis of variation of ocean floor bathymetry and heat flow with age, *J. Geophys. Res.*, 82, 803–827, doi:10.1029/JB082i005p00803.

Pelayo, A. M., S. Stein, and C. A. Stein (1994), Estimation of oceanic hydrothermal heat flux from heat flow and depths of midocean ridge seismicity and magma chambers, *Geophys. Res. Lett.*, 21, 713–716, doi:10.1029/94GL00395.

Purdy, G. M., L. S. L. Kong, G. L. Christeson, and S. C. Solomon (1992), Relationship between spreading rate and the seismic structure of mid-ocean ridges, *Nature*, 355, 815–817, doi:10.1038/355815a0.

Ramondenc, P., N. G. A. Leonid, K. L. Von Damm, and R. P. Lowell (2006), The first measurements of hydrothermal heat output at 9° 50′N, East Pacific Rise, *Earth Planet. Sci. Lett.*, 245, 487–497, doi:10.1016/j.epsl.2006.03.023.

Sclater, J. G., C. Jaupart, and D. Galson (1980), The heat flow through oceanic and continental crust and the heat loss of the Earth, *Rev. Geophys.*, 18, 269–311, doi:10.1029/RG018i001p00269.

Sohn, R. A., D. J. Fornari, K. L. V. Damm, J. A. Hildebrand, and S. C. Webb (1998), Seismic and hydrothermal evidence for a cracking event on the East Pacific Rise crest at 9°50′N, *Nature*, 396, 159–161, doi:10.1038/24146.

Sohn, R. A., J. A. Hildebrand, and S. C. Webb (1999), A microearthquake survey of the high-temperature vent fields on the volcanically active East Pacific Rise, *J. Geophys. Res.*, 104, 25,367–25,377, doi:10.1029/1999JB900263.

Spinelli, G. A., E. R. Giambalvo, and A. T. Fisher (2004), Sediment permeability, distribution, and influence on fluxes in oceanic basement, in *Hydrogeology of the Oceanic Lithosphere*, edited by E. E. Davis and H. Elderfield, pp. 151–188, Cambridge Univ. Press, New York.

Stein, C. A., and S. Stein (1993), Constraints on Pacific midplate swells from global depth-age and heat flow-age models, in *The Mesozoic Pacific: Geology, Tectonics, and Volcanism*, *Geophys. Monogr. Ser.*, vol. 77, edited by M. S. Pringle, pp. 53–76, AGU, Washington, D. C.

Stein, C. A., and S. Stein (1994), Constraints on hydrothermal heat flux through the oceanic lithosphere from global heat flow, *J. Geophys. Res.*, 99, 3081–3095, doi:10.1029/93JB02222.

Stein, C. A., S. Stein, and A. Pelayo (1995), Heat flow and hydrothermal circulation, in *Seafloor Hydrothermal Systems*, *Geophys. Monogr. Ser.*, vol. 91, edited by S. Humphris et al., pp. 425–445, AGU, Washington, D. C.

Tivey, M. A., and H. P. Johnson (2002), Crustal magnetization reveals subsurface structure of Juan de Fuca Ridge hydrothermal vent fields, *Geology*, 30, 979–982, doi:10.1130/0091-7613(2002)030<0979:CMRSSO>2.0.CO;2.

Toomey, D. R., S. C. Soloman, and G. M. Purdy (1988), Microearthquakes beneath the median valley of the Mid-Atlantic Ridge near 23°N: Tomography and tectonics, *J. Geophys. Res.*, 93, 9093–9112, doi:10.1029/JB093iB08p09093.

VanTongeren, J. A., P. B. Kelemen, and K. Hanghoj (2008), Cooling rates in the lower crust of the Oman ophiolite: Ca in olivine, revisited, *Earth Planet. Sci. Lett.*, 267, 69–82, doi:10.1016/j.epsl.2007.11.034.

Von Herzen, R. P., and S. Uyeda (1963), Heat flow through the eastern Pacific Ocean floor, *J. Geophys. Res.*, 68, 4219–4250.

Wilcock, W. S. D., and J. R. Delaney (1996), Mid-ocean ridge sulfide deposits: Evidence for heat extraction from magma chambers or cracking fronts?, *Earth Planet. Sci. Lett.*, 145, 49–64, doi:10.1016/S0012-821X(96)00195-1.

Wilcock, W. S. D., S. D. Archer, and G. M. Purdy (2002), Microearthquakes on the Endeavour segment of the Juan de Fuca Ridge, *J. Geophys. Res.*, 107(B12), 2336, doi:10.1029/2001JB000505.

Williams, D. L., R. P. Von Herzen, J. G. Sclater, and R. N. Anderson (1974), The Galapagos spreading centre: Lithospheric cooling and hydrothermal circulation, *J. R. Astron. Soc.*, 38, 587–608.

Wolery, T. J., and N. H. Sleep (1976), Hydrothermal circulation and geochemical flux at mid-ocean ridges, *J. Geol.*, 84, 249–275, doi:10.1086/628195.

R. N. Harris, College of Oceanic and Atmospheric Science, Oregon State University, Corvallis, OR 97331, USA.

G. A. Spinelli, Earth and Environmental Science Department, New Mexico Institute of Mining and Technology, Socorro, NM 87801, USA. (spinelli@nmt.edu)